*Revue Roumaine de Chimie,* **2008**, *53*(12), 1131–1140

# ELECTROCHEMICAL AND SPECTRAL STUDY OF THE REDOX BEHAVIOR AND CARDIOTOXICITY OF ANTICANCER DRUGS WITH ANTRAQUINONE STRUCTURE: QUINIZARIN

Alina LATUS [a] and Elena VOLANSCHI [b*]

[a] Institute of Physical Chemistry "I. Murgulescu", Romanian Academy, Splaiul Independentei 202, Bucharest, RO-060021 ROUMANIA
[b] Department of Physical Chemistry, University of Bucharest Blvd Elisabeta 4-12, Bucharest, RO-030018 ROUMANIA

*Received March 20, 2008*

1,4-dihydroxyanthraquinone (quinizarin) is the simplest molecule, which represents the structure of the specific chromophore for some biological and pharmaceutical compounds, being the main part in the chemical structure of daunorubicin, doxorubicin, and mitoxantrone.
The present paper investigates the behavior in reduction and oxidation processes of quinizarin in aprotic neutral and basic media by coupled electrochemical and spectral techniques (*in-situ* techniques), including absorption spectroscopy, in order to identify the intermediate species and to propose a reaction mechanism. The influence of electrogenerated bases (EGB) was investigated by comparison with the spectroelectrochemistry in presence of added tetrabutylammonium hydroxide (TBOH). The proposed reaction sequences are supported by Digisim 3.03 simulations.
Semiempirical MO-calculations were performed to determine the electronic structural features implied in reduction and oxidation processes and to analyze the energetics of the electron transfer (ET) from different reduction intermediates to molecular oxygen.

## INTRODUCTION

The anthracycline antibiotics doxorubicin and daunorubicin are used in the treatment of various malignancies including leukemia, non-Hodgkin's lymphoma, and breast cancer. Their antitumoral action is due to the intercalation of the anthracycline aromatic moiety between the DNA base pairs, resulting in the inhibition of transcription by blockage of RNA polymerase.[1,2] But, besides their positive action, these drugs possess also an undesirable cardiotoxicity. The generally accepted mechanism for the cardiotoxicity of the anthracyclines implies the mono or bielectronic reduction of the drug, with the appearance of reactive reduction intermediates, radical species which may mediate electron transfer to molecular oxygen, with formation of superoxide anion radicals, responsible for cellular damage and cardiotoxicity.[3, 4]

1, 4-dihydroxyanthraquinone (quinizarin) is the simplest molecule, which represents the structure of the specific chromophore for some biological and pharmaceutical compounds; it is the main part in the chemical structure of daunorubicin, doxorubicin, and mitoxantrone.[5,6] Quinizarin is accredited with properties that span from being employed as a dye, a photoinitiator and an additive in lubricants.[7] The structure of quinizarin has been a subject of numerous spectroscopic investigations, including fluorescence studies, resonance Raman and infrared spectroscopy,[8,9] and X-ray crystallographic investigations.[10]

The purpose of the present paper is to investigate the behavior in redox processes of quinizarin in both aprotic and protic media by coupled electrochemical and spectral techniques (*in-situ* techniques), including absorption spectroscopy, in order to identify the intermediate species and to propose a reaction mechanism. Semiempirical PM3 MO-calculations were performed to determine the electronic structural features implied in redox processes. The electron transfer from different reduction intermediates to molecular oxygen was also analyzed.

* Corresponding author: elenavolanschi@gmail.com

## RESULTS AND DISCUSSION

### A. Cyclic Voltammetry

The cyclic voltammetry (CV) of a quinizarin solution ($5 \times 10^{-3}$ M) in deaerated DMSO, at different sweep rates (0.05÷1.0) V/s in the range 0 to -1.8 V (Fig. 1), evidenced two redox couples, assigned to two successive reduction steps of quinizarin.

The first process is characterized by: difference between cathodic and anodic peak potential, $\Delta E_p$, in the range 151-370 mV for both couples and the ($i_{pa}/i_{pc}$) ratio slightly smaller than unity (0.70 ÷ 0.85) suggesting a slow follow-up chemical reaction, most probably a protonation by the water traces always present in the commercially available solvent. The thermodynamic and kinetic parameters obtained by direct analysis were refined by Digisim simulations using the default values for the electron transfer parameter and diffusion coefficient, and the resulting simulations are presented in Fig. 1A.

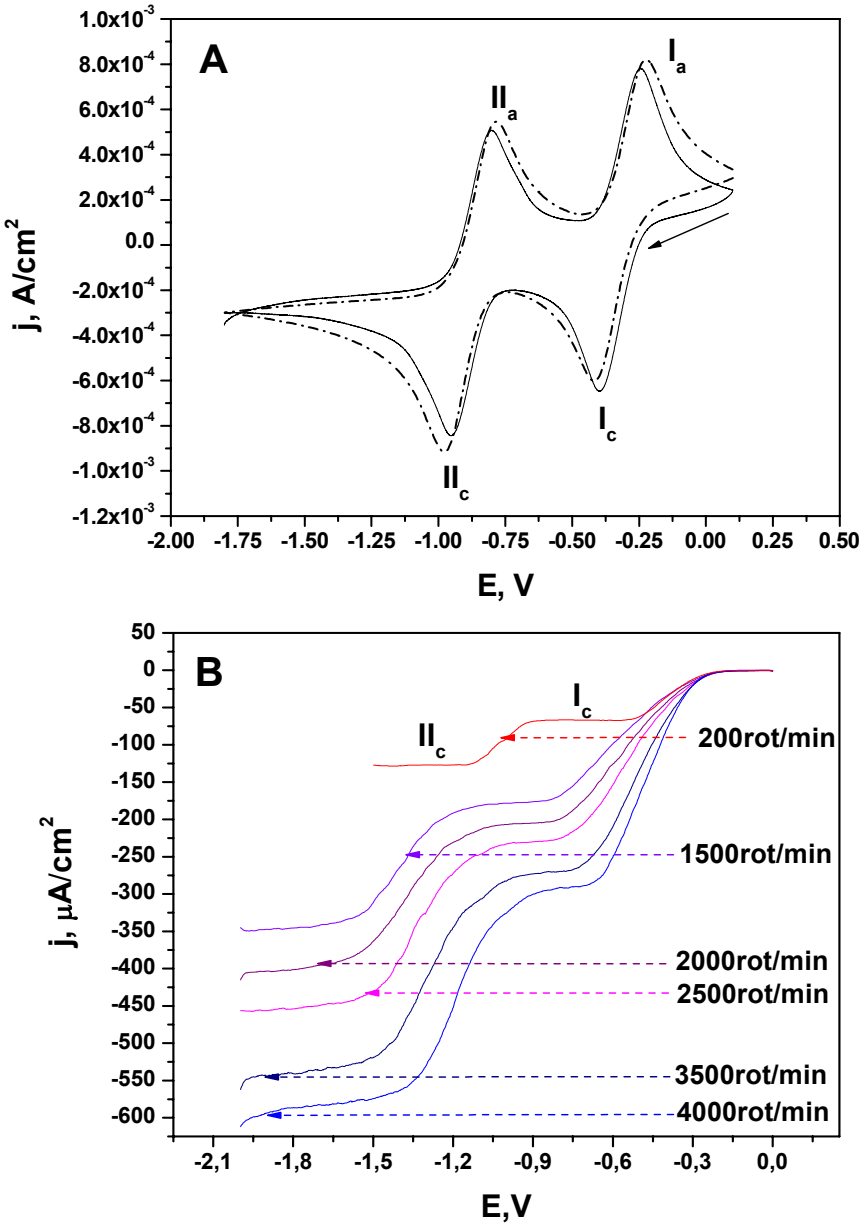


Fig. 1 – (A) Cyclic voltammogram of quinizarin ($5 \times 10^{-3}$ M) in DMSO / 0.1M TBAP at sweep rate 0.05 V/s. *Full line* – experimental; *dashed line* – simulated with: $k_s^I = k_s^{II} = 10^{-3}$ cm/s, $\alpha$=0.50, $E^0_I$ = -0.32 V, $E^0_{II}$ = -0.88 V, $D_0=10^{-5}$ cm$^2$ /s; (B) RDE of the first two waves of quinizarin solution ($2.6 \times 10^{-3}$ M) in DMSO / 0.1M TBAP at sweep rate 0.02 V/s and different rotation rates.

The analysis of the RDE curves in Fig. 1B shows that the both ET are mono electronic. The plot $E = E_{1/2} + \frac{RT}{nF}\ln\frac{i_{lc} - i}{i - i_{la}}$, (N = 10, r = 0.99) gives $E_{1/2}^{I}$ = -0.37 V, $E_{1/2}^{II}$ = -1.01 V; the Levich plot $i_{lc} = 0.62 \cdot nFAD_O^{2/3}\varpi^{1/2} \cdot \nu^{-1/6} \cdot c_o^*$ (N = 20, r = 0.99) allows to determine $D_O$, in the range $(1 \div 3.3) \times 10^{-6}$ cm$^2$/s.

These results are in agreement with cyclic voltammetry data. Therefore, the electrochemical reduction of quinizarin (denoted in the followings as $AH_2$ due to the two dissociable phenolic groups) in DMSO may be accounted by two successive electron transfers (EE), leading to the anion-radical and dianion, respectively:

$$AH_2 + e^- \rightleftarrows AH_2^{\bullet -}$$
$$AH_2^{\bullet -} + e^- \rightleftarrows AH_2^{2-}$$

If the reduction of hydroquinones has long been regarded as an excellent example of a simple two-step cathodic reduction,[11] the same thing cannot be said about the oxidation processes. Currently, a lot of research is done in the last years in order to find the most probable mechanism, which is important to understand biochemical processes such as cytotoxic functions and antitumor activity. [12-14]

The CV of quinizarin starting with oxidation is presented in Fig. 2, in the potential range -0.75 to +1.6 V. At scan rates up to 0.2 V/s an asymmetric oxidation wave (wave III) is apparent, most probably corresponding to the irreversible bielectronic oxidation of the hydroquinone moiety of quinizarin, leading to a diquinone, A:

$$AH_2 \longrightarrow A + 2e^- + 2H^+$$

The electrochemical analysis of wave III indicates a slow electrochemical process. The large values of the slope peak potential versus the logarithm of scan rate, $\partial E_{pa}^{III}/\partial(\log v) \sim 180$ mV/dec and the peak width ($E_p - E_{p/2}$) of about 100 mV, are consistent with transfer coefficient values $\alpha$ slightly lower than 0.5. [15]

On the reverse scan the wave $IV_c$, the less intense couple V and the reversible couple corresponding to the first reduction step of the starting compound (couple I), are apparent.

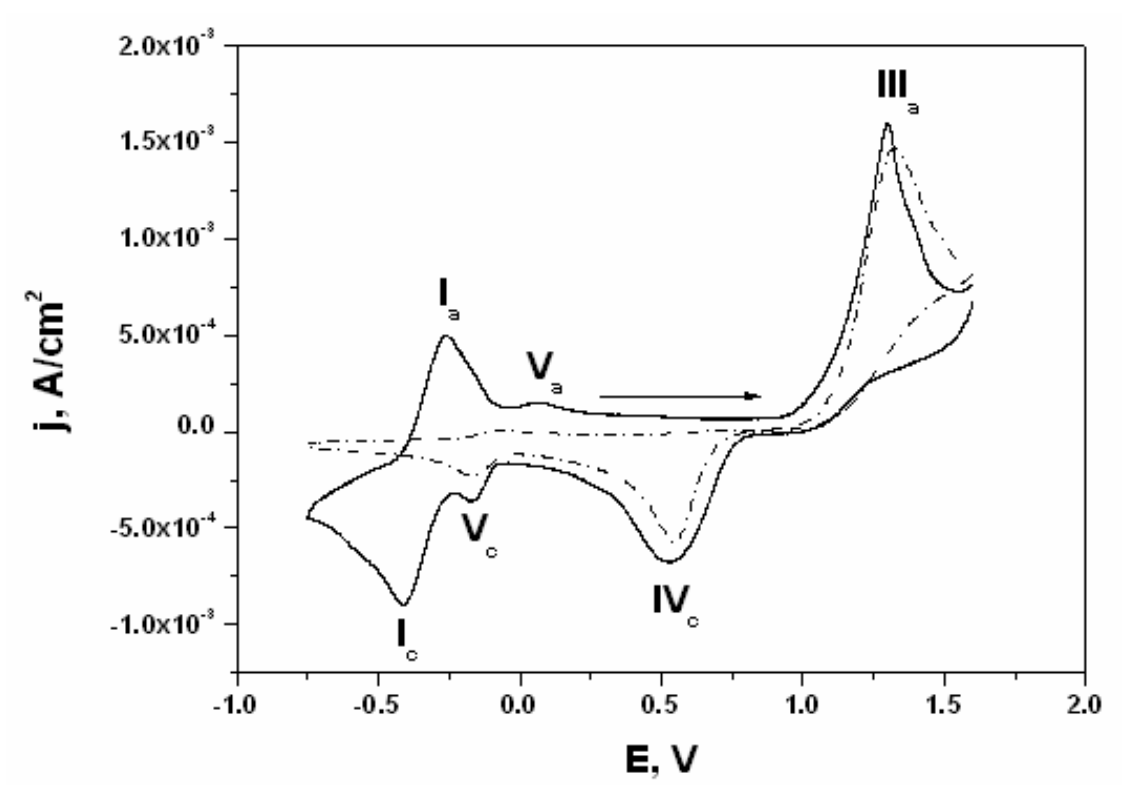


Fig. 2 – Cyclic voltammogram of quinizarin ($5 \times 10^{-3}$ M) in DMSO / 0.1M TBAP at sweep rate 0.05 V/s. *Full line* – experimental; *dashed line* – simulated with the mechanism and parameters in the text. The simulation does not include the first reduction couple of the starting compound (couple I) because of the limitation of the Digisim 3.03 program, which allows only 3 electron transfers.

Recent work on the electrochemical oxidation of hydroquinone in acetonitrile[16] has shown that the bielectronic oxidation of this compound corresponds in fact to an ECE mechanism, the two successive electron transfers being connected by a chemical step, corresponding to the acid dissociation of the cation radical resulted from the first ET, $AH_2^+$.

Taking into account our cyclic voltammetry results and literature data, the oxidation process of quinizarin may be represented by the following reaction sequence, analyzed by Digisim simulation, with the default values of $D_O$ and α.

(1) $AH_2 \rightleftarrows AH_2^{\bullet+} + e^-$ **(E)** $E^0_{III} = 0.86$ V $k_s = 10^{-5}$ cm·s$^{-1}$

(2) $AH_2^{\bullet+} \rightleftarrows AH^\bullet + H^+$ **(C)** $K_{eq} = 500$ M $k_f = 10$ s$^{-1}$

(3) $AH^\bullet \rightleftarrows AH^+ + e^-$ **(E)** $E^0_{III} = 0.86$ V $k_s = 10^{-5}$ cm·s$^{-1}$

(4) $AH^+ \rightleftarrows A + H^+$ **(C)** $K_{eq} = 100$ M $k_f = 10$ s$^{-1}$

(5) $A + e^- \rightleftarrows A^{\bullet-}$ **(E)** $E^0_V = -0.12$ V $k_s = 10^{-2}$ cm·s$^{-1}$

The Digisim simulation accounts for the cyclic voltammetry results in Fig. 2. The cation radical obtained in the first oxidation step is expected to be a strong acid (by comparison with hydroquinone in DMSO, with $pK_a$ = -8.1[17]) and therefore, at small scan rates, the intermediate species $AH^\bullet$ is accumulated in the neighborhood of the electrode. The species $AH^\bullet$ is oxidated to $AH^+$ at a potential close to that of wave III, and therefore either two distinct waves or an asymmetric one are apparent. On the reverse scan, both intermediates $AH^\bullet$ and $AH^+$ are reduced at the potential of wave IV. At the same time, formation of the diquinone A (step 4) is favored. The final product of oxidation, diquinone A is reduced, as expected, at a less negative potential that the substrate, accounting for the small redox couple ($E_{pc}^V/E_{pa}^V$), present before the redox couple of the starting compound, couple I. At high sweep rates, a smaller quantity of diquinone A is formed and therefore its reduction couple is covered by the first redox couple of the substrate. The evolution of the intensity ratio of waves IV and V with the scan rate on the simulations (data not shown) supports this mechanism. Species $AH^+$ formed in step 3, is expected to be less acidic than $AH_2^{\bullet+}$, it means that the formation of the diquinone A (step 4) will not be favored at high scan rates, which explains the small intensity ratio $I_{pc}^V / I_{pc}^{IV}$ in these conditions.

This mechanism is also supported by the CV of a quinizarin solution ($2.6 \times 10^{-3}$ M) in the presence of tetrabutylammonium hydroxide (TBOH) (0.08M) in DMSO at a sweep rate of 0.05 V/s (Fig. 3).

In presence of small amounts of base, the equilibrium in step 2 is shifted towards the dissociated forms. Consequently, the two oxidation waves collapse in a single wave III, corresponding to the global reaction (steps 1-3): $AH_2 \rightarrow AH^+ + 2e^- + H^+$

Moreover, at a 1:1 molar ratio (Fig. 3A), wave IV is split into two mono electronic waves ($AH^+ + e^- \rightarrow AH^\bullet$ and $AH^\bullet + e^- \rightarrow AH^-$) and, on the second anodic scan, wave VI is apparent, corresponding to the reversible couple present in the system: $AH^\bullet + e^- \rightarrow AH^-$.

This behavior is also sustained by the dependence of the peak potential of wave IV on the concentration of TBOH (Fig.3B). For concentrations lower than corresponding to 1:1 molar ratio, the peak potential is strongly pH dependent, the predominant intermediate species being $AH^+$, formed in the previous ECE sequence (steps 1-3), and reduced at a more positive potential than $AH^\bullet$.

In the 1:1 TBOH/substrate molar ratio concentrations range, the peak potential of wave IV is independent of pH, and the bielectronic wave is split into two mono electronic waves (Fig. 3A, B), corresponding to the reduction of $AH^+$ to $AH^\bullet$ and $AH^\bullet$ to $AH^-$, respectively. With increasing TBOH concentration, step 4 is also favored, and the redox couple V, corresponding to the process: $A + e^- \rightarrow A^{\bullet-}$ is more intense (Fig. 3A).

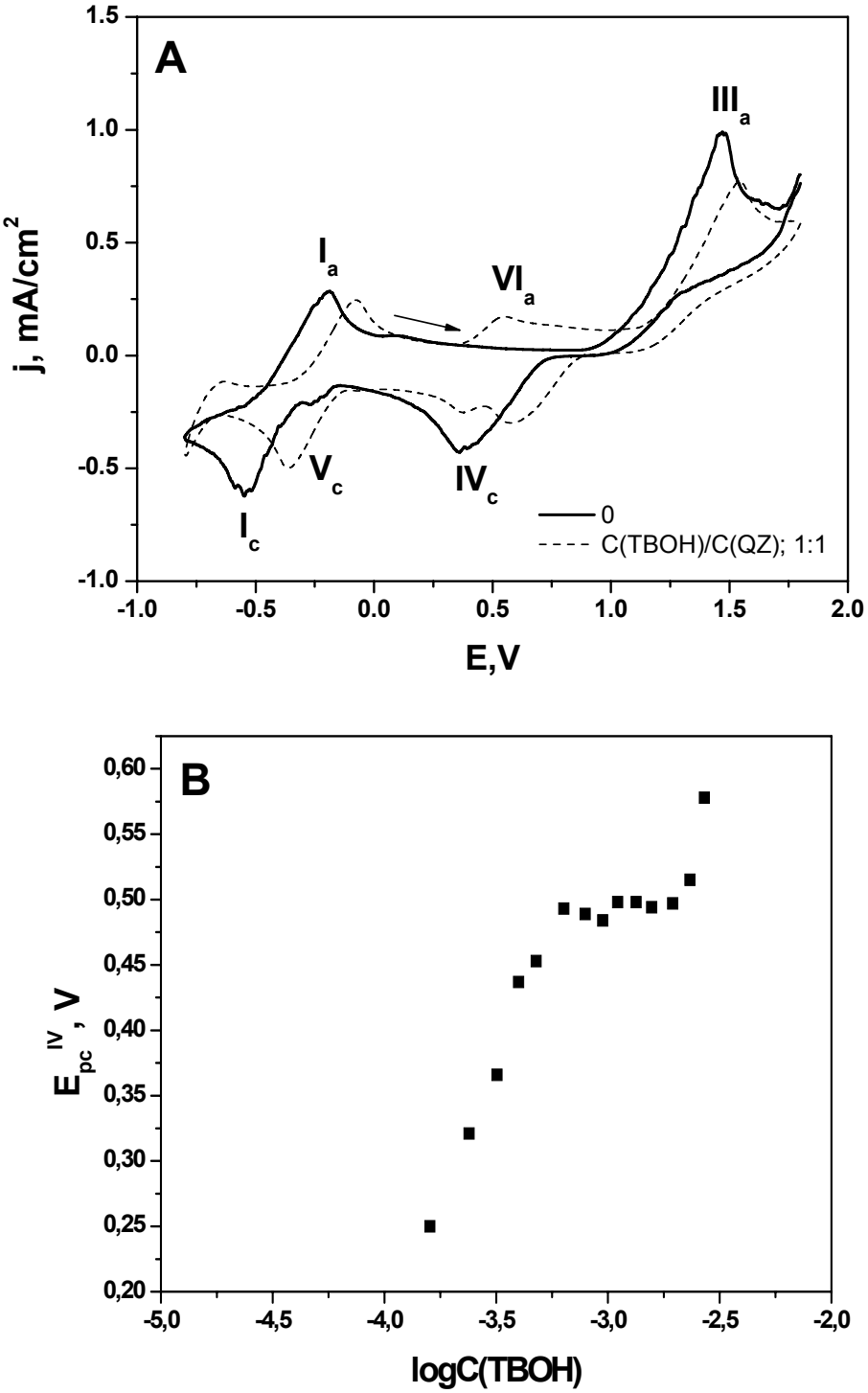


Fig. 3 – (A) Cyclic voltammogram of quinizarin solution ($2.6 * 10^{-3}$ M) in the absence (full line) and presence (dashed line) of TBOH (1:1) molar ratio. (B) Dependence of the peak potential of wave IV, $E_{pc}^{IV}$ on the TBOH concentration.

### B. Absorption spectra

In order to get a deeper insight into the reduction mechanism of quinizarin, optical spectra were performed during the chemical and electrochemical reduction using *in-situ* techniques. The family of curves obtained at the electrochemical reduction of quinizarin in DMSO at a potential corresponding to the first wave on the cyclic voltammogram (Fig. 4A).

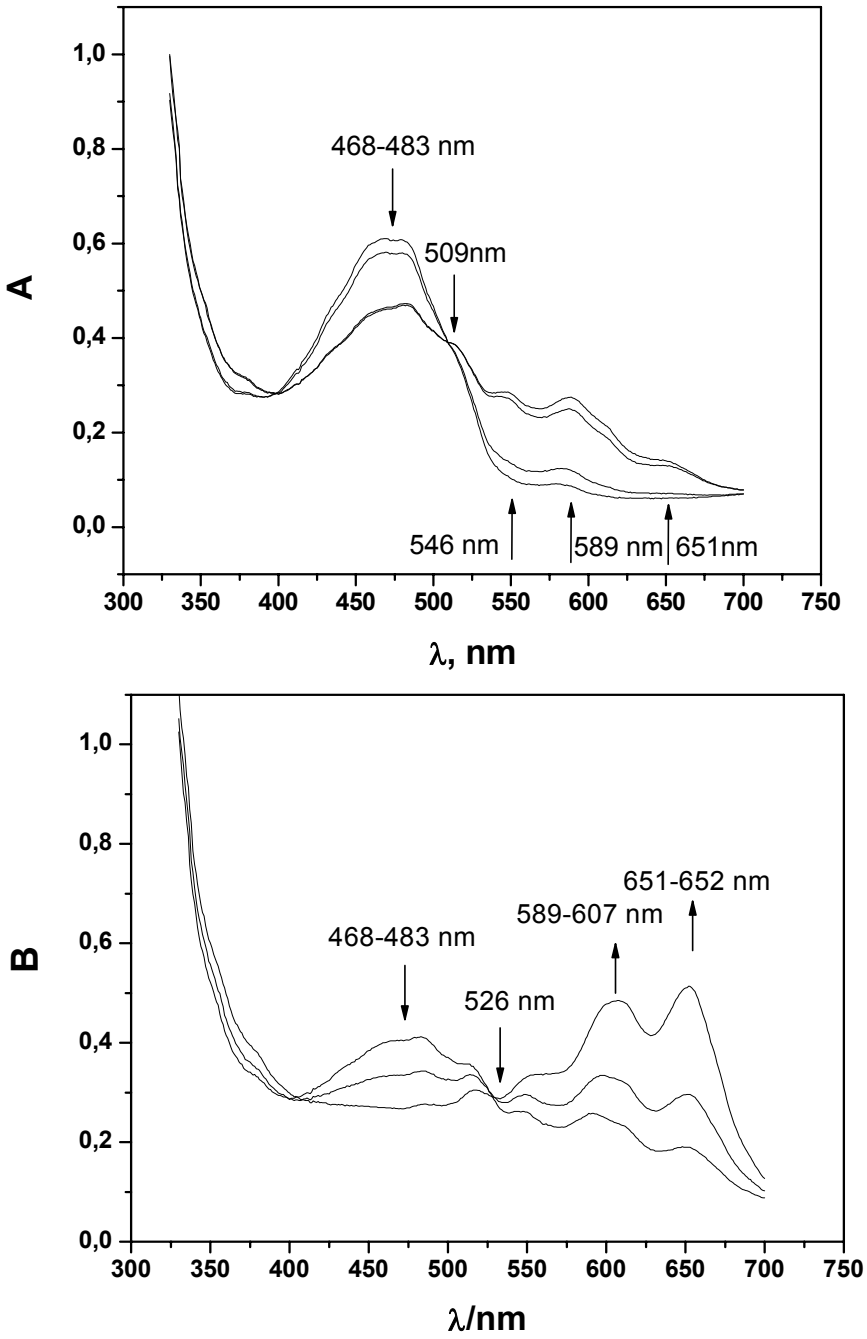


Fig. 4 – (A) Absorption spectra recorded at the electrolysis of quinizarin solution ($5.28 \times 10^{-5}$ M) in DMSO / 0.1M TBAP at the potential of the first reduction couple after 0, 3, 15, 18 min. of electrolysis; (B) Prolonged electrolysis (21, 30, 35 min.) at -0.5 V.

The absorption band of the starting compound is located at 476 nm.[5, 18] During the electrolysis at the potential of the first reduction wave on the voltammogram, this band decreases in time and a new absorption band with maxima at 546 and at 589 nm are apparent, with an isobestic point around 509 nm. At this level the process is reversible, the initial compound being entirely recovered on air or at electrochemical oxidation. Therefore, the new bands at 546 and 589 nm were assigned respectively to the anion-radical ($AH_2^{\bullet -}$) and to the anion ($AH^-$), formed by the acid dissociation of the substrate under the influence of the electrogenerated bases (EGB). When the electrolysis is prolonged (after 25 minutes) and the solution of quinizarin is opened to air, the bands at 546 and 589 nm decrease and the absorption band of the initial compound is only partially recovered (Fig. 4B). The beginning of this irreversible process is characterized by the increase of the band at 651-652 nm, which corresponds to a new species.

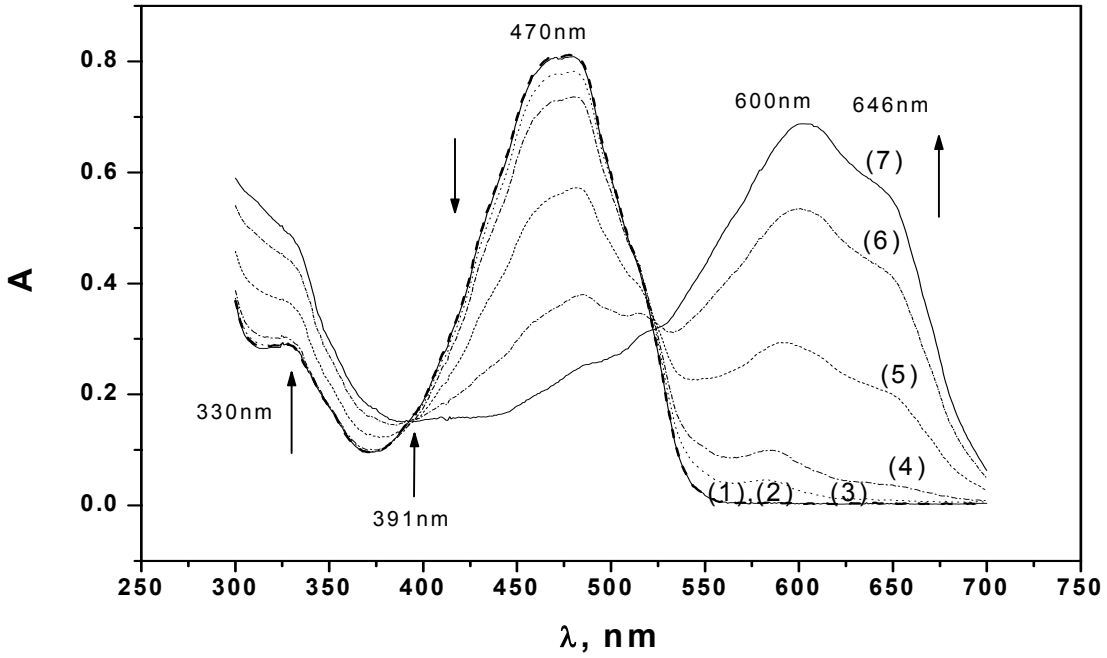


Fig. 5 – UV - VIS spectra of quinizarin solution ($5.28 \times 10^{-5}$ M) in DMSO in the presence of different concentrations of TBOH (0.008 M) corresponding to $C_{TBOH}$ / $C_{Qz}$ molar ratios: (1) – 0; (2) – 0.76; (3) – 3.03; (4) – 4.55; (5) – 6.06; (6) – 7.58; (7) – 9.09.

A similar behavior is observed in the presence of TBOH (Fig. 5) and outlines the role of electrogenerated bases (EGB), anion radical $AH_2^-$, anion $AH^-$, and dianion $AH_2^{2-}$.

The family of curves obtained is similar to that observed on electrochemical reduction. The new bands, increasing with the TBOH concentration are assigned to the anion ($AH^-$, the band at 600 nm) and dianion ($A^{2-}$, the band at 330 nm),[5] formed by the dissociation of the phenolic groups of quinizarin, according to the equilibria:

$$AH_2 + OH^- \rightleftarrows AH^- + H_2O$$

$$AH_2 + 2OH^- \rightleftarrows A^{2-} + 2H_2O$$

By acidifying the solution with water, the band of the starting compound is recovered, meaning that the process is reversible when C (TBOH)/C (Qz) < 2. The band at 646 nm, the increase of which is marking the irreversible character of the process, was tentatively assigned to the diquinone A, obtained by the air oxidation of the alkaline solution.

Corroborating these results, the following redox mechanism is proposed:

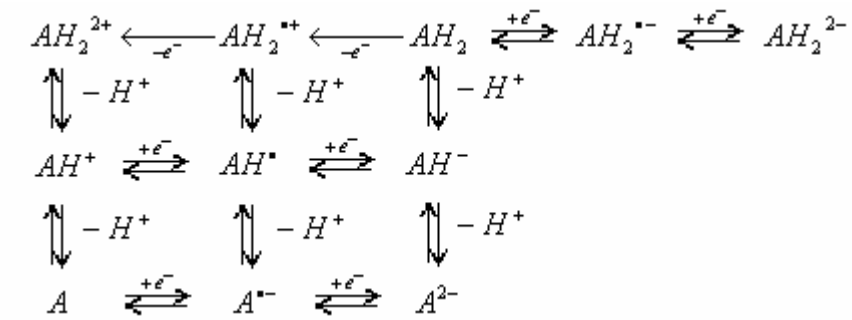


In the above scheme the electron transfer processes (horizontal lines) and the proton transfer steps (vertical lines) of quinizarin were characterized by their thermodynamic and kinetic parameters and the intermediate species involved were identified either by cyclic voltammetry and/or

by absorption spectroscopy, in aprotic neutral and basic media.

### C. MO calculations

Antibiotics with the structure of anthraquinone introduce out of their antitumoral activity, a cardiac toxicity, restricting their clinical use. The molecular mechanism of cardiotoxicity is not well understood, but it seems to be connected with the possibility of electron transfer from the reduced intermediates to the molecular oxygen having as result the appearance of molecular oxygen reactive species, responsible for the damage of biological macromolecules.

MO-calculations can give necessary information to understand, at molecular level, the characteristics of electronic structure, responsible for the reactivity in redox processes. The calculations were performed for quinizarin and for its product of oxidation, diquinone. The electron parameters used in the discussion of the reactivity in redox processes are:[19, 20] the ionization potential given by Koopman's theorem by, $IP = -\varepsilon_{homo}$; the absolute electronegativity, $\chi_V = (IP + EA) / 2 = -1/2\ (\varepsilon_{homo} + \varepsilon_{lumo})$; the adiabatic ionisation potential, $IP_{ad}$ defined as ΔH for the reaction : $A \rightarrow A + e^-$; the adiabatic electron affinity, $EA_{ad}$ defined as the negative of ΔH for the reaction: $A + e^- \rightarrow A^-$; the adiabatic electronegativity, $\chi_{ad} = 1/2\ (IP_{ad} + EA_{ad})$.

The results are presented in Table 1. For the neutral molecule a geometry corresponding to the most stable conformer of quinizarin with formation enthalpies of -107.81 kcal/mol was considered. In this conformer the -OH groups of cycle B are orientated towards the oxygen atoms, being involved in intramolecular hydrogen bonding. The hydrogen bonding stabilizes the anion radical and the values of potential $E^{0'}$ are moved towards less negative values in comparison with anthraquinone: (-0.320 V) *vs* (-0.595 V).

For diquinone, higher electron affinities and lower LUMO orbitals energies are obtained in respect with quinizarin. These results are correlated with the reduction potential of the first redox couple. The adiabatic and absolute electronegativities are close to one another, what means that there is no significant geometry modification of molecules in redox processes. The analysis of frontier orbitals implicated in redox process shows that both highest occupied (HOMO) and lowest unoccupied (LUMO) molecular orbitals are π-type orbitals.

*Table 1*

PM 3- calculated electronic parameters of quinizarin (Qz) and diquinone (Dq) implied in redox processes

| Compound | ΔH (kcal/mol) | $\varepsilon_{homo}$ (eV) | $\varepsilon_{lumo}$ (eV) | $\chi_V$ (eV) | $IP_{ad}$ (kcal/mol) | $EA_{ad}$ (kcal/mol) | $\chi_{ad}$ (eV) | $E^{0'}$ (V) |
|---|---|---|---|---|---|---|---|---|
| **Qz** | -107.81 | -8.99 | -1.69 | 5.34 | 191.88 | 49.59 | 5.25 | -0.320 |
| **Dq** | -60.95 | -10.46 | -2.12 | 6.29 | 231.25 | 63.23 | 6.40 | -0.253 |

The HOMO orbital is mainly delocalized on the substituted cycle of quinizarin (cycle A) (Fig. 6), meaning that this moiety is involved in oxidation processes, leading to diquinone. The LUMO orbital is mainly delocalized on the central cycle (cycle B), meaning that this part of the molecule is involved in reduction processes.

The reactivity of intermediate species of quinizarin towards molecular oxygen was analyzed for both states of oxygen: the fundamental triplet state ($^3\Sigma_g$) and the singlet state ($^1\Delta_g$).

The results in Table 2 show that for quinizarin the electron transfer from the radical anion towards molecular oxygen is not energetically favorable in both triplet and singlet states, while the electron transfer from the dianion is energetically favorable for both states of oxygen (especially for the state of singlet).

In the case of the product of oxidation of quinizarin, diquinone, the electron transfer from dianion $A^{2-}$ towards molecular oxygen is energetically favorable for both states of oxygen (especially for the singlet state), whereas the electron transfer from radical anion $A^{\bullet -}$ towards molecular oxygen is not energetically favorable.

The reactions for diquinone are more endotherm than those of quinizarin, what means that even if the diquinone is more reducible, the activation of molecular oxygen by $A^{\bullet -}$ and $A^{2-}$ is less probable than for quinizarin. Comparison of the results in Table 2 with the calculated enthalpy variations of mitoxantrone [21] reveals that ET reactions from the anion radical ($AH_2^{\bullet -}$) and

dianion ($AH_2^{2-}$) of quinizarin to both singlet and triplet states of oxygen are more favorable energetically for quinizarin, predicting a lower cardiac toxicity for mitoxantrone. This is in agreement with literature data revealing the smaller tendency of mitoxantrone to participate to the redox cycling in cardiac mitochondria, being less effective in producing free radicals in comparison with the others antitumorals drugs,[22,23] and is probably due to the 5, 8 - amino substituents of this drug.

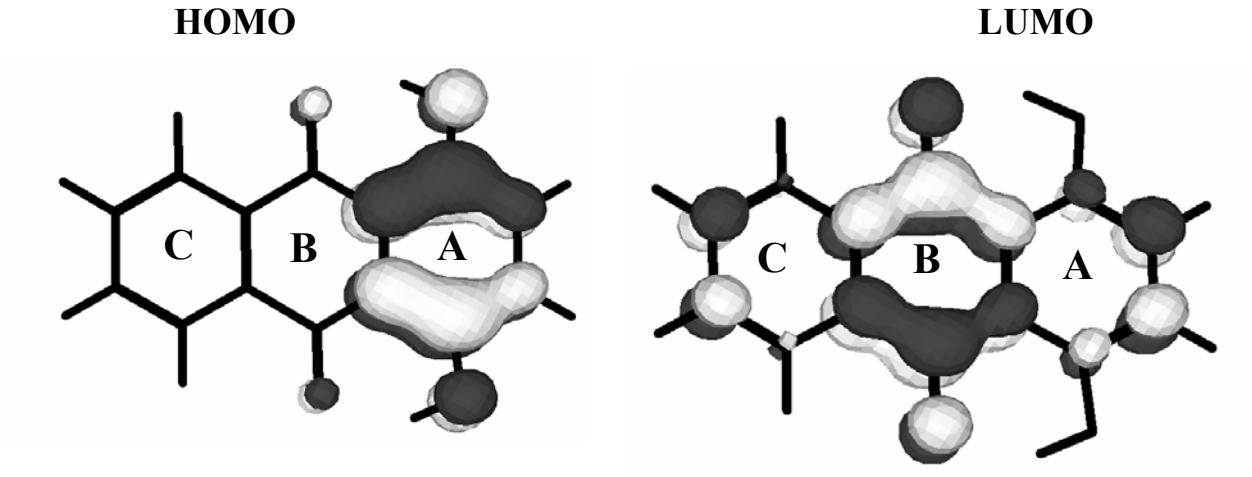


Fig. 6 – The shape of the frontier molecular orbitals (HOMO and LUMO) of quinizarin.

*Table 2*

Enthalpy variation ($\Delta^rH$) for the ET reactions of intermediate reduction species of quinizarin ($AH_2$) and diquinone (A) to molecular oxygen

| Reaction | $O_2$ [a] | $\Delta^rH$ (kcal/mol) [b] (gas phase) |
|---|---|---|
| $AH_2^{\bullet-} + O_2 \rightarrow AH_2 + O_2^{\bullet-}$ | $^1\Delta_g$ | 17.94 |
| | $^3\Sigma_g$ | 40.49 |
| $AH_2^{2-} + O_2 \rightarrow AH_2^{\bullet-} + O_2^{\bullet-}$ | $^1\Delta_g$ | -75.02 |
| | $^3\Sigma_g$ | -52.46 |
| $A^{\bullet-} + O_2 \rightarrow A + O_2^{\bullet-}$ | $^1\Delta_g$ | 31.58 |
| | $^3\Sigma_g$ | 54.14 |
| $A^{2-} + O_2 \rightarrow A^{\bullet-} + O_2^{\bullet-}$ | $^1\Delta_g$ | -69.95 |
| | $^3\Sigma_g$ | -47.39 |

[a] For molecular oxygen the $\Delta H^f$ values for the gas phase were used: -4.18 ($^3\Sigma_g$), 18.38 ($^1\Delta_g$), for $O_2^{\bullet-}$: -13.27 kcal/mol.
[b] $\Delta^rH = \Sigma\ \Delta H^f_{Prod.} - \Sigma\ \Delta H^f_{React.}$

In conclusion, the present work is a tentative approach of understanding the redox processes of the drugs with anthraquinone structure at a molecular level. The analysis of the cardiotoxicity by estimation of the thermodynamic parameters of the ET reactions from the reduction and/or oxidation intermediates of these drugs to molecular oxygen gives only an approximate evaluation of

this toxicity, being based on vacuum MO calculations. Better results are expected by taking into account the influence of solvent, and are in progress in our laboratory.

## EXPERIMENTAL

Quinizarin was purchased from Aldrich (96%) and used without additional purification. Stock solutions of quinizarin were prepared in dimethyl sulphoxide (DMSO), due to insolubility. The perclorate tetra buthyl ammonium (TBAP) 0.1M was employed as supporting electrolyte.

Cyclic voltammetry (CV) experiments with both stationary and rotating disc electrode (RDE) were performed at a VOLTLAB-40 electrochemical laboratory, with carbon working electrode, platinum – counter electrode and SCE and Ag-quasi reference electrode. The optical spectra were registered during electrochemical and chemical reduction using *in-situ* techniques on a UV-VIS spectrophotometer, α-Helios UNICAM, and a potentiostat Radelkis. Experimental results were analyzed by software ORIGIN 7.5 and compared with parameters found by simulation, accomplished by the software DIGISIM 3.03. Semi empirical molecular orbital calculations were performed using the MOPAC 6.0 program package, the PM3 hamiltonian, EF (eigenvector following) algorithm of optimization and computer software HyperChem-6. The calculations were performed on in vacuo isolated molecules, and do not take into account the influence of the solvent.

## REFERENCES


1. Y. Yoshikawa, K. Yoshikawa and T. Kanbe, *Biophys. Chem.*, **1996**, *61*, 93-100.
2. D. A. Gewirtz, *Biochem.Pharmacol.*, **1999**, *57*, 727-41.
3. J.W. Lown, "Reactive Oxygen Species in Chemistry, Biology and Medicine", A. Quintanilha (Ed.), Plenum Press, New York, 1988, p. 167-185.
4. J.W. Lown, "Anthracycline and anthracenedione-based anticancer drugs", Elsevier, Amsterdam, 1988.
5. G. Fabriciova, J.V. Garcia-Ramos, P. Miskovsky and S. Sanchez-Cortes, *Vibr. Spectr.*, **2004**, *34*, 273–281.
6. D. Jancura, S. Sanchez-Cortes, E. Kocisova, A. Tinti, P. Miskovsky and A. Bertoluzza, *Biospectroscopy*, **1995**, *1*, 265-273.
7. R. S. Bottei and D. A. Lusardi, *Thermochim. Acta*, **1981**, *43*, 355-363.
8. G. Smulevich, L. Angeloni, S. Giovannardi and M. P. Marzocchi, *Chem. Phys.*, **1982**, *65*, 313-322.
9. P. K. Dutta and B. S. Lee, *J. Raman Spectrosc.,* **1988**, *19*, 175-178.
10. G. D. Nigam and B. Deppisch, *Zeit. Kristal.*, **1980**, *151*, 185-191.
11. M. W. Lehmann and D. H. Evans, *J. Electroanal. Chem.*, **2001**, *500*, 12–20.
12. R. J. Driebergen, J. den Hartigh, J. J. M. Holthuis, A. Hulshoff, W. J. van Oort, S. J. Postma Kelder, W. Verboom, D. N. Reinhoudt, M. Bos and W. E. van der Linden, *Anal. Chim. Acta*, **1990**, *233*, 251-268.
13. T. J. Monks, R. P. Hanzlik, G. M. Cohen, D. Ross and D. G. Graham, *Toxicol. Appl. Pharmacol.*, **1992**, *112*, 2-16.
14. A. E. Alegria, E. Cordones, G. Santiago, Y. Marcano, S. Sanchez, M. Gordaliza and M. L. Martin-Martin, *Toxicol*, **2002**, *175*, 167-175.
15. A. J. Bard and R. L. Faulkner, "Electrochimie. Principes, methodes et applications", Masson, Paris, 1983, p. 239-271.
16. P. D. Astudillo, J. Tiburcio and F. J. Gonzalez, *J. Electroanal. Chem.*, **2007**, *604*, 57-64.
17. F. G. Bordwell and J. P. Cheng, *J. Am. Chem. Soc*., **1991**, *113*, 1736-1743.
18. M. Hovaneissian, P. Archier and C. Vieillescazes, *Dyes and Pigments*, **2007**, *74*, 706-712.
19. A. Sawyer, E. Sullivan and Y. H. Miriam, *J. Comp. Chem.*, **1996**, *17*, 204-225.
20. Y. H. Miriam and A. Sawyer, *J. Comp. Aid. Molec. Des.*, **1996**, *10*, 441-460.
21. M. Enache, C. Bendic and E. Volanschi, *Bioelectrochemistry*, **2008**, *72*, 10-20.
22. J. H. Doroshow and K. J. A. Davies*, J. Biol. Chem.*, **1986**, *261*, 3068–3074.
23. B. Nguyen and P. L. Gutierrez, *Chem. Biol. Interact.*, **1990**, *74*, 139–162.